Weak charge form factor and radius of ^{208}Pb through parity violation in electron scattering

C. J. Horowitz[*]

University of Tennessee, Knoxville, Tennesee 37996, and Indiana University, Bloomington, Indiana 47405, USA

Z. Ahmed, C.-M. Jen, A. Rakhman, and P. A. Souder

Syracuse University, Syracuse, New York 13244, USA

M. M. Dalton, N. Liyanage, K. D. Paschke, K. Saenboonruang, and R. Silwal

University of Virginia, Charlottesville, Virginia 22903, USA

G. B. Franklin, M. Friend, and B. Quinn

Carnegie Mellon University, Pittsburgh, Pennsylvania 15213, USA

K. S. Kumar, D. McNulty,[†] L. Mercado, S. Riordan, and J. Wexler

University of Massachusetts Amherst, Amherst, Massachusetts 01003, USA

R. W. Michaels

Thomas Jefferson National Accelerator Facility, Newport News, Virginia 23606, USA

G. M. Urciuoli

INFN, Sezione di Roma, I-00161 Rome, Italy

We use distorted wave electron scattering calculations to extract the weak charge form factor $F_W(\bar{q})$, the weak charge radius R_W, and the point neutron radius R_n of ^{208}Pb from the Lead Radius Experiment (PREX) parity-violating asymmetry measurement. The form factor is the Fourier transform of the weak charge density at the average momentum transfer $\bar{q} = 0.475 \, \text{fm}^{-1}$. We find $F_W(\bar{q}) = 0.204 \pm 0.028$ (exp) ± 0.001 (model). We use the Helm model to infer the weak radius from $F_W(\bar{q})$. We find $R_W = 5.826 \pm 0.181$ (exp) ± 0.027 (model) fm. Here the experimental error includes PREX statistical and systematic errors, while the model error describes the uncertainty in R_W from uncertainties in the surface thickness σ of the weak charge density. The weak radius is larger than the charge radius, implying a "weak charge skin" where the surface region is relatively enriched in weak charges compared to (electromagnetic) charges. We extract the point neutron radius $R_n = 5.751 \pm 0.175$ (exp) ± 0.026 (model) ± 0.005 (strange) fm from R_W. Here there is only a very small error (strange) from possible strange quark contributions. We find R_n to be slightly smaller than R_W because of the nucleon's size. Finally, we find a neutron skin thickness of $R_n - R_p = 0.302 \pm 0.175$ (exp) ± 0.026 (model) ± 0.005 (strange) fm, where R_p is the point proton radius.

PACS number(s): 21.10.Gv, 25.30.Bf, 24.80.+y, 27.80.+w

Parity-violating elastic electron scattering provides a model-independent probe of neutron densities, because the weak charge of a neutron is much larger than the weak charge of a proton [1]. In the Born approximation, the parity-violating asymmetry A_{pv}, the fractional difference in cross sections for positive and negative helicity electrons, is proportional to the weak form factor F_W. This is very close to the Fourier transform of the neutron density. Therefore the neutron density can be extracted from an electroweak measurement [1]. However, one must include the effects of Coulomb distortions, which have been accurately calculated [2], if the charge density ρ_{ch} [3] is well known. Many details of a practical parity-

violating experiment to measure neutron densities, along with a number of theoretical corrections, were discussed in a long paper [4].

Recently, the Lead Radius Experiment (PREX) measured A_{pv} for 1.06-GeV electrons, scattered by about 5 deg from ^{208}Pb, and the neutron radius R_n was extracted [5]. To do this, the experimental A_{pv} was compared to a least squares fit of R_n as a function of A_{pv}, predicted by seven mean-field models [6] (see also [7]). In the present paper, we provide a more detailed analysis of the measured A_{pv}. This analysis provides additional information, such as the weak form factor, and clarifies the (modest) model assumptions necessary to extract R_n.

We start with distorted wave calculations of A_{pv} for an electron moving in Coulomb and weak potentials [2]. We use these to extract the weak form factor from the PREX measurement. In the Born approximation, one can determine the weak form factor directly from the measured A_{pv}. However,

---

[*]horowit@indiana.edu

[†]Present address: Idaho State University, Pocatello, Idaho 83209, USA.

Coulomb distortions may make A_{pv} sensitive to the weak form factor for a range of momentum transfers q. In addition, the experimental acceptance for PREX includes a range of momentum transfers for laboratory scattering angles from about 3.5 to 8 deg [5]. Therefore we need to make very modest assumptions about the shape of the weak form factor (how it depends on momentum transfer q) in order to determine the value of the form factor at the average momentum transfer $\bar{q}$ [5],

$$\bar{q} = \langle Q^2 \rangle^{1/2} = 0.475 \pm 0.003 \text{ fm}^{-1}. \tag{1}$$

We initially assume the weak charge density of ^{208}Pb, $\rho_W(r)$, has a Wood-Saxon form,

$$\rho_W(r) = \frac{\rho_0}{1 + \exp[(r - R)/a]}, \tag{2}$$

with parameters ρ_0, R, and a. Note that this form is used only to access the sensitivity to the shape of the form factor and our results will be independent of this assumed form. The weak density is normalized to the weak charge $Q_W = \int d^3r \rho_W(r)$; see below.

We define the weak form factor $F_W(q)$ as the Fourier transform of $\rho_W(r)$,

$$F_W(q) = \frac{1}{Q_W} \int d^3r \frac{\sin qr}{qr} \rho_W(r). \tag{3}$$

This is normalized $F_W(q = 0) = 1$. Our procedure is to calculate $A_{pv}(\theta)$, including full Coulomb distortions [2], assuming ρ_W from Eq. (2). We average $A_{pv}(\theta)$ over laboratory scattering angle θ using the experimental acceptance $\epsilon(\theta)$ [5],

$$\langle A \rangle = \frac{\int d\theta \sin \theta \, \epsilon(\theta) \frac{d\sigma}{d\Omega} A_{pv}}{\int d\theta \sin \theta \, \epsilon(\theta) \frac{d\sigma}{d\Omega}}. \tag{4}$$

Here the unpolarized elastic cross section is $\frac{d\sigma}{d\Omega}$. We then adjust R until the calculated $\langle A \rangle$ agrees with the PREX result [5]

$$A_{pv}^{\text{Pb}} = 0.656 \pm 0.060 \text{ (stat)} \pm 0.014 \text{ (syst) ppm}. \tag{5}$$

Here the first error is statistical and the second error includes systematic contributions. For $a = 0.6$ fm, we obtain a central value of $R = 6.982$ fm; see below. Finally from the $\rho_W(r)$ in Eq. (2), which reproduces A_{pv}^{Pb}, we calculate $F_W(\bar{q})$ using Eq. (3). This procedure fully includes Coulomb distortions and depends slightly on the assumed surface thickness a in Eq. (2). In Table I we show Wood-Saxon fits to the seven nonrelativistic and relativistic mean-field model weak charge densities considered in Ref. [6]. Note that these models span a very large range of neutron radii R_n. The average value of a for these models is 0.61 ± 0.05 fm. Using a central value of $a = 0.6$ fm, we obtain

$$F_W(\bar{q}) = 0.204 \pm 0.028 \text{ (exp)} \pm 0.001 \text{ (mod)}. \tag{6}$$

Here the first experimental error is from adding the statistical and systematic errors in Eq. (5) in quadrature. The second model error is from varying a by ± 0.05 fm. This shows that the extracted form factor is all but independent of the assumed shape of the weak charge density. Equation (6) is a major result

TABLE I. Least squares fits of Wood Saxon (R, a, see Eq. (2)) or Helm model (R_0, σ, see Eq. (8)) parameters to theoretical mean field model weak charge densities.

Mean field force	Wood Saxon		Helm	
	R (fm)	a (fm)	R_0 (fm)	σ (fm)
Skyrme I [8]	6.655	0.564	6.792	0.943
Skyrme III [9]	6.820	0.613	6.976	1.024
Skyrme SLY4 [10]	6.700	0.668	6.888	1.115
FSUGold [11]	6.800	0.618	6.961	1.028
NL3 [12]	6.896	0.623	7.057	1.039
NL3p06 [6]	6.730	0.606	6.886	1.010
NL3m05 [6]	7.082	0.605	7.231	1.012
Average		0.61 ± 0.05		1.02 ± 0.09

of this paper. This is the form factor of the weak charge density that is implied by the PREX measurement.

We now explore some of the implications of Eq. (6) using the Helm model [13] for the weak form factor. In the past, the Helm model has proven very useful for analyzing (unpolarized) electron scattering form factors [14,15]; see also Ref. [16] for an application of the Helm model to neutron rich nuclei. The weak charge density is first assumed to be uniform out to a diffraction radius R_0. This uniform density is then folded with a Gaussian of width σ to get the final weak density. The width σ includes contributions from both the surface thickness of the point nucleon densities and the single-nucleon form factor. In the Helm model, the weak form factor has a very simple form,

$$F_W(q) = \frac{3}{qR_0} j_1(qR_0) e^{-\sigma^2 q^2/2}, \tag{7}$$

with $j_1(x) = \sin x/x^2 - \cos x/x$ a spherical Bessel function. The diffraction radius R_0 determines the location q_0 of the zero in the weak form factor $F_W(q_0) = 0$. In coordinate space, the Helm model weak charge density can be written in terms of error functions (erf),

$$\rho_W(r) = \frac{3Q_W}{8\pi R_0^3} \left\{ \text{erf}\left(\frac{R_0 + r}{\sqrt{2}\sigma}\right) - \text{erf}\left(\frac{r - R_0}{\sqrt{2}\sigma}\right) \right.$$
$$\left. + \sqrt{\frac{2}{\pi}} \frac{\sigma}{r} \left(e^{-\frac{1}{2}(\frac{r+R_0}{\sigma})^2} - e^{-\frac{1}{2}(\frac{r-R_0}{\sigma})^2} \right) \right\}. \tag{8}$$

The root-mean-square (rms) radius of the weak charge density R_W (or weak radius) is $R_W^2 = \int d^3r \, r^2 \rho_W(r)/Q_W$,

$$R_W^2 = \frac{3}{5} (R_0^2 + 5\sigma^2). \tag{9}$$

We see that Eq. (6) implies via Eq. (7) a relationship between allowed values of R_0 and σ. This relationship then implies via Eq. (9) a range of weak radii. Thus Eq. (6) does not, by itself, determine the weak radius. In principle the rms radius follows from the derivative of the form factor with respect to Q^2 at $q = 0$. Because the PREX measurement is at finite q, one needs to assume some information about the surface thickness σ in order to extract R_W. Alternatively within the Helm model, if one determined the location of the zero

of the form factor q_0 in addition to Eq. (6), then this would uniquely fix both R_0 and σ and so determine R_W.

In Table I we collect values of σ determined by least squares fits of the Helm density, Eq. (8), to seven model mean-field densities. The average of σ for the seven mean-field densities is 1.02 fm, and individual results deviate by no more than 0.09 fm from this average. If one assumes $\sigma = 1.02 \pm 0.09$ fm, Eqs. (6), (7), and (9) imply

$$R_W = 5.826 \pm 0.181 \,(\text{exp}) \pm 0.027 \,(\text{mod}) \text{ fm.} \qquad (10)$$

Again the larger experimental (exp) error is from adding the statistical and systematic errors in Eq. (5) in quadrature, while the model (mod) error comes from the *coherent* sum of the assumed ± 0.09 fm uncertainty in σ and the ± 0.001 model error in F_W. The model error in Eq. (10) provides an estimate of the uncertainty in R_W that arises because of uncertainties in the surface thickness. Of course, it is not guaranteed that all theoretical models will have a surface thickness within the range 1.02 ± 0.09 fm. Nevertheless, this result suggests that uncertainties in surface thickness are much less important for R_W than either the present PREX experimental error or even that of an improved measurement where the experimental error is reduced by about a factor of three [17]. This is consistent with earlier results of Furnstahl [18], suggesting a nearly unique relation between $F_W(\bar{q})$ and the point neutron radius R_n. We emphasize that if uncertainties in the surface thickness are a concern, one should compare theoretical predictions for the form factor $F_W(\bar{q})$ to Eq. (6), instead of comparing theoretical predictions for R_W to Eq. (10).

Comparing Eq. (10) to the experimental charge radius $R_{\text{ch}} = 5.503$ fm [3,19] implies a "weak charge skin" of thickness

$$R_W - R_{\text{ch}} = 0.323 \pm 0.181 \,(\text{exp}) \pm 0.027 \,(\text{mod}) \text{ fm.} \qquad (11)$$

Thus the surface region of ^{208}Pb is relatively enhanced in weak charges compared to electromagnetic charges. This weak charge skin is closely related to the expected neutron skin; see below. Equation (11) itself represents an experimental milestone. We now have direct evidence that the weak charge density, of a heavy nucleus, is more extended than the electromagnetic charge density.

In Fig. 1 we show a Helm model weak charge density that is consistent with the PREX measurement. This figure shows an uncertainty range from the experimental error and a model uncertainty from the assumed ± 0.09 fm uncertainty in σ. Parameters for these densities are presented in Table II. We also show in Fig. 1 the (electromagnetic) charge density [3] and a typical mean-field weak charge density based on the FSUGold interaction; see Eq. (17). This theoretical density is within the error bars of the Helm model density.

Finally we wish to extract R_n for ^{208}Pb from R_W in Eq. (10). We start by reviewing the relationship between the point proton radius R_p and the measured charge radius R_{ch}. Ong *et al.* have [20]

$$R_{\text{ch}}^2 = R_p^2 + \langle r_p^2 \rangle + \frac{N}{Z} \langle r_n^2 \rangle + \frac{3}{4M^2} + \langle r^2 \rangle_{\text{so}}. \qquad (12)$$

Here the charge radius of a single proton is $\langle r_p^2 \rangle = 0.769$ fm^2 and that of a neutron is $\langle r_n^2 \rangle = -0.116$ fm^2. We calculate
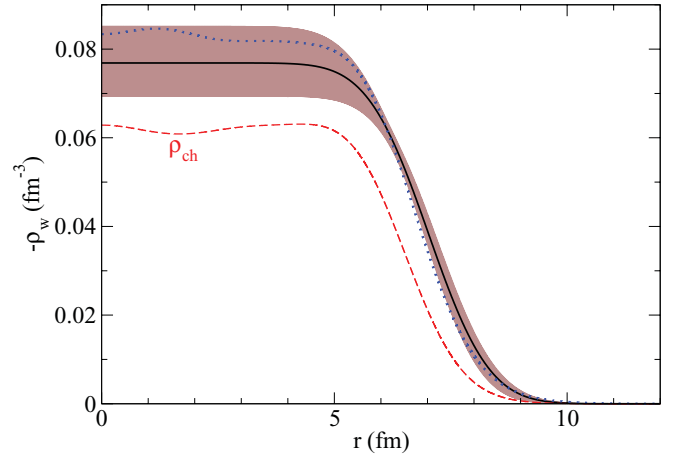

FIG. 1. (Color online) Helm model weak charge density $-\rho_W(r)$ of ^{208}Pb that is consistent with the PREX result (solid black line). The brown (gray) error band shows the incoherent sum of experimental and model errors. The red dashed curve is the experimental (electromagnetic) charge density ρ_{ch} and the blue dotted curve shows a sample mean-field result based on the FSUGold interaction [11].

that the contribution of spin-orbit currents to R_{ch} is small because of cancelations between protons and neutrons $\langle r^2 \rangle_{\text{so}} = -0.028$ fm^2. Finally the Darwin contribution $3/4M^2$ is also small, with M being the nucleon mass. For ^{208}Pb we have $R_{\text{ch}}^2 = R_p^2 + 0.5956$ fm^2, or, for $R_{\text{ch}} = 5.503$ fm [3,19],

$$R_p = 5.449 \text{ fm.} \qquad (13)$$

For the weak charge density of a spin-zero nucleus, we neglect meson exchange and spin-orbit currents and write [4]

$$\rho_W(r) = 4 \int d^3r' \left[G_n^Z(|\mathbf{r} - \mathbf{r}'|)\rho_n(r') + G_p^Z(|\mathbf{r} - \mathbf{r}'|)\rho_p(r') \right]. \qquad (14)$$

Here the density of weak charge in a single proton $G_p^Z(r)$ or neutron $G_n^Z(r)$ is the Fourier transform of the nucleon (electric) Sachs form factors $G_p^Z(Q^2)$ and $G_n^Z(Q^2)$. These describe the coupling of a Z^0 boson to a proton or neutron [4],

$$4G_p^Z = q_p G_E^p + q_n G_E^n - G_E^s, \qquad (15)$$

$$4G_n^Z = q_n G_E^p + q_p G_E^n - G_E^s. \qquad (16)$$

At tree level, the weak nucleon charges are $q_n^0 = -1$ and $q_p^0 = 1 - 4\sin^2\Theta_W$. We include radiative corrections by using the values $q_n = -0.9878$ and $q_p =$

TABLE II. Helm model weak charge density parameters R_0 and σ that reproduce the following values for the weak form factor $F_W(\bar{q})$; see Eqs. (6) and (7).

Density	R_0 (fm)	σ (fm)	$F_W(\bar{q})$
Central value	7.167	1.02	0.204
Exp error bar	7.417	1.02	0.176
Exp error bar	6.926	1.02	0.232
Model error bar	7.137	1.11	0.203
Model error bar	7.194	0.93	0.205

0.0721 based on the up C_{1u} and down C_{1d} quark weak charges in Refs. [21,22]. The Fourier transform of the proton (neutron) electric form factor is $G_E^p(r)$ [$G_E^n(r)$] and has total charge $\int d^3r\, G_E^p(r) = 1$ [$\int d^3r\, G_E^n(r) = 0$]. Finally G_E^s describes strange quark contributions to the nucleon's electric form factor [23–26]. Note that there may be some small uncertainty regarding the Q^2 dependence of the radiative corrections. This uncertainty could change R_n^2 (see below) by a very small amount of order $(1 + q_n)\langle r_p^2 \rangle$.

Equation (14) can be rewritten by using a similar expression for ρ_{ch}

$$\rho_W(r) = q_p\,\rho_{\text{ch}}(r) + \int d^3r' \big[q_n\big(G_E^p\rho_n + G_E^n\rho_p\big) - G_E^s\rho_b\big] \tag{17}$$

with $\rho_b = \rho_n + \rho_p$. The weak charge of ^{208}Pb is

$$Q_W = \int d^3r\,\rho_W(r) = Nq_n + Zq_p = -118.55. \tag{18}$$

From Eq. (17) we relate the point neutron rms radius R_n to R_W,

$$R_n^2 = \frac{Q_W}{q_n N}R_W^2 - \frac{q_p Z}{q_n N}R_{\text{ch}}^2 - \langle r_p^2\rangle - \frac{Z}{N}\langle r_n^2\rangle + \frac{Z+N}{q_n N}\langle r_s^2\rangle, \tag{19}$$

where $\langle r_s^2\rangle = \int d^3r'\,r'^2 G_E^s(r')$ is the square of the nucleon strangeness radius. This yields

$$R_n^2 = 0.9525 R_W^2 - 1.671\langle r_s^2\rangle + 0.7450 \text{ fm}^2. \tag{20}$$

The strangeness radius of the nucleon $\langle r_s^2\rangle^{1/2}$ is constrained by experimental data [23–26] and their global analysis [27,28]. Using Table V of Ref. [28] for $Q^2 < 0.11$ GeV^2 gives $\langle r_s^2\rangle = -6 dG_E^s/dQ^2 = 0.02 \pm 0.04 \approx \pm 0.04$ fm^2.

The neutron radius then follows from Eq. (10),

$$R_n = 5.751 \pm 0.175 \text{ (exp)} \pm 0.026 \text{ (mod)} \pm 0.005 \text{ (str) fm.} \tag{21}$$

Here the very small third (str) error is from possible strange quark contributions. The neutron radius R_n is slightly smaller than R_W because of the nucleon's size. Finally, the neutron skin thickness is

$$R_n - R_p = 0.302 \pm 0.175 \text{ (exp)} \pm 0.026 \text{ (mod)}$$
$$\pm 0.005 \text{ (str) fm.} \tag{22}$$

This result agrees, within the model error, with the result of Ref. [5], $R_n - R_p = 0.33^{+0.16}_{-0.18}$ fm. The small difference between the present result and that of Ref. [5] arises because of small limitations of the Helm model in representing theoretical mean-field densities. For example, the Helm model does not have the correct exponential behavior at large distances. However, we have clarified how the extraction of the neutron radius depends upon assumptions on the weak skin thickness σ and we provide an explicit model error for the uncertainty in $R_n - R_p$ because of uncertainties in σ.

We now summarize our results. In this paper we use distorted wave electron scattering calculations for ^{208}Pb to extract the weak charge form factor $F_W(\bar{q})$, Eq. (6), the weak radius R_W, Eq. (10), and the point neutron radius R_n, Eq. (21), from the PREX parity-violating asymmetry measurement. The weak form factor is the Fourier transform of the weak charge density at the average momentum transfer of the experiment. This quantity is essentially model independent and is insensitive to assumptions about the surface thickness.

The extraction of R_W depends on modest assumptions about the surface thickness. We use the Helm model to derive an estimate on the uncertainty in R_W because of the uncertainty in surface thickness. We find a "weak charge skin" where the surface region is relatively enriched in weak charges compared to electromagnetic charges. This is closely related to the neutron skin where R_n is larger than the point proton radius R_p. Finally, we extract R_n, given R_W, and find it to be slightly smaller than R_W because of the nucleon's size.

[1] T. W. Donnelly, J. Dubach, and Ingo Sick, Nucl. Phys. A **503**, 589 (1989).

[2] C. J. Horowitz, Phys. Rev. C **57**, 3430 (1998).

[3] B. Frois *et al.*, Phys. Rev. Lett. **38**, 152 (1977).

[4] C. J. Horowitz, S. J. Pollock, P. A. Souder, and R. Michaels, Phys. Rev. C **63**, 025501 (2001).

[5] S. Abrahamyan *et al.* (PREX Collaboration), Phys. Rev. Lett. **108**, 112502 (2012).

[6] S. Ban, C. J. Horowitz, and R. Michaels, J. Phys. G **39**, 015104 (2012).

[7] X. Roca-Maza, M. Centelles, X. Vinas, and M. Warda, Phys. Rev. Lett. **106**, 252501 (2011).

[8] D. Vautherin and D. M. Brink, Phys. Rev. C **5**, 626 (1972).

[9] M. Beiner, H. Flocard, N. Van Giai, and P. Quentin, Nucl. Phys. A **238**, 29 (1975).

[10] E. Chabanat, P. Bonche, P. Haensel, J. Meyer, and R. Schaeffer, Nucl. Phys. A **635**, 231 (1998).

[11] B. G. Todd-Rutel and J. Piekarewicz, Phys. Rev. Lett. **95**, 122501 (2005).

[12] G. A. Lalazissis, J. Konig, and P. Ring, Phys. Rev. C **55**, 540 (1997).

[13] R. H. Helm, Phys. Rev. **104**, 1466 (1956).

[14] M. Rosen, R. Raphael, and H. Uberall, Phys. Rev. **163**, 927 (1967).

[15] R. Raphael and M. Rosen, Phys. Rev. C **1**, 547 (1970).

[16] S. Mizutori, J. Dobaczewski, G. A. Lalazissis, W. Nazarewicz, and P. G. Reinhard, Phys. Rev. C **61**, 044326 (2000).

[17] P. A. Souder *et al.*, [http://hallaweb.jlab.org/parity/prex/prexII.pdf].

[18] R. J. Furnstahl, Nucl. Phys. A **706**, 85 (2002).

[19] G. Fricke *et al.*, in *Springer Materials: The Landolt-Bornstein Database*, edited by H. Schoopper. [http://www.springermaterials.com].

[20] A. Ong, J. C. Berengut, and V. V. Flambaum, Phys. Rev. C **82**, 014320 (2010).

[21] J. Erler, A. Kurylov, and M. J. Ramsey-Musolf, Phys. Rev. D **68**, 016006 (2003).

[22] K. Nakamura *et al.*, J. Phys. G **37**, 075021 (2010).

[23] R. D. McKeown, Phys. Lett. B **219**, 140 (1989); D. T. Spayde *et al.*, *ibid.* **583**, 79 (2004); T. Ito *et al.*, Phys. Rev. Lett. **92**, 102003 (2004).

[24] K. A. Aniol *et al.*, Phys. Lett. B **509**, 211 (2001); Phys. Rev. C **69**, 065501 (2004); Phys. Rev. Lett. **96**, 022003 (2006); Phys. Lett. B **635**, 275 (2006); A. Acha *et al.*, Phys. Rev. Lett. **98**, 032301 (2007); Z. Ahmed *et al.*, arXiv:1107.0913 [nucl-ex].

[25] D. H. Beck, Phys. Rev. D **39**, 3248 (1989); D. S. Armstrong *et al.*, Phys. Rev. Lett. **95**, 092001 (2005); D. Androic *et al.*, *ibid.* **104**, 012001 (2010).

[26] F. E. Maas *et al.*, Phys. Rev. Lett. **93**, 022002 (2004); **94**, 152001 (2005); S. Baunack *et al.*, *ibid.* **102**, 151803 (2009).

[27] R. D. Young, J. Roche, R. D. Carlini, and A. W. Thomas, Phys. Rev. Lett. **97**, 102002 (2006).

[28] J. Liu, R. D. McKeown, and M. J. Ramsey-Musolf, Phys. Rev. C **76**, 025202 (2007).